

# SOIL CARBON STOCKS UNDER PASTURES IN THE BRAZILIAN CERRADO REGION THEIR ASSESSMENT BY ORBITAL REMOTE SENSING

G.G.Szakács<sup>1,\*</sup>, V.Eschenbrenner<sup>2</sup>, C.C. Cerri<sup>1</sup>, M. Bernoux<sup>2</sup>

<sup>1</sup> Laboratory of Environmental Biogeochemistry - Center of Nuclear Energy in Agriculture (CENA/USP)  
CP 96, 13400-970 Piracicaba, Brazil – (\*gabor@cena.usp.br)

<sup>2</sup> UR041 – SeqC, Institut de Recherche pour le Développement (IRD), Montpellier, France

**Key Words:** Climate, Agriculture, Soil, Estimation, Landsat, Spectral

## ABSTRACT:

The article 3.4 of the Kyoto Protocol acknowledges agriculture soils as a potential sink for soil organic carbon (SOC). To estimate current and potential SOC on a broad scale for these potential sinks in a fast and inexpensive manner, the applicability of orbital remote sensing techniques was studied. Four pastures on sandy soils of the Brazilian Cerrado were chosen due to their SOC sequestration potential. Thereupon, the four chosen pastures were characterized in terms of their SOC (0-50cm). Subsequently was investigated the correlation degree between SOC and Leaf Area Index (LAI) and SOC and pasture reflectance in 6 different spectra in the range from 450nm – 2350nm, using the Enhanced Thematic Mapper (ETM+) sensor of satellite Landsat 7. The SOC showed a good correlation with the LAI ( $r = 0,97$ ). As exists a good correlation between LAI and Spectral Vegetation Indices (SVIs), the good correlation between SOC and LAI permits an adequate estimation for current and potential SOC through the NDVI.

A regression analysis showed also particularly good correlations between SOC and pasture reflectance in the red ( $r = 0,96$ ) and shortwave infrared (SWIR) ( $r = 0,95$ ) spectrum. Both methods, the orbital measured LAI and the direct reflectance approach, seem to be a promising tool to estimate current and potential SOC by orbital remote sensing.

## KURZFASSUNG:

Der Artikel 3.4 des Kyoto Protokolls hebt hervor, dass landwirtschaftlich genutzte Böden potentielle Fixierer von Bodenkohlenstoff darstellen. Um den aktuellen und potentiellen Bodenkohlenstoffgehalt grossflächig, schnell und kostengünstig ermitteln zu können, wurde für diesen Zweck die Eignung der orbitalen Fernerkundung analysiert. Es wurden aus Gründen des Kohlenstofffixierungspotentials vier Weideflächen im Brasilianischen Cerrado untersucht. Es wurde die Korrelation zwischen Bodenkohlenstoff /Blattoberflächenindex und Bodenkohlenstoff/Weideflächenreflexion untersucht. Zur Spektralanalyse wurden sechs Spektralbänder des Satelliten Landsat 7 herangezogen, welche den Spektralbereich von 450nm - 2350nm umfassen. Der Bodenkohlenstoff zeigte eine gute Korrelation mit dem Blattoberflächenindex. Da es eine gute Korrelation zwischen Blattoberflächenindex und spektralen Vegetationsindexen (z.B. NDVI) gibt, kann daraus abgeleitet werden, dass aktuelle und potentielle Bodenkohlenstoffgehalte mittels orbitaler Fernerkundung ermittelt werden können.

Zudem zeigte eine lineare Regressionsanalyse zwischen Bodenkohlenstoffgehalten und Weidereflexion besonders gute Korrelationen im roten ( $r = 0,96$ ) und mittleren Infrarotbereich ( $r = 0,95$ ) und qualifiziert auch den Ansatz der Bodenkohlenstoffbestimmung mittels Weidereflexion als geeignet.

## 1. INTRODUCTION

The signature of the “United Nations Framework Convention on Climate Change” (UNFCCC) of Brazil and 150 other countries in Rio de Janeiro in June 1992 indicated the wide acknowledgement that climate changes are representing a major threat for the environment and the economic development in the world. Climate changes are caused by an increasing greenhouse effect, above the desired level. CO<sub>2</sub> has the biggest impact of all greenhouse gases with a global warming potential of 60% (IPCC, 2000). The main goal of the Kyoto Protocol is the slowing of human contribution in relation to the increasing atmospheric concentrations of CO<sub>2</sub> (Walsh, 1999). Therefore, the Kyoto Protocol acknowledges the possibility of SOC sequestration in cultivated soils (art° 3.4). The protocol also promotes research for SOC estimation in a quick, inexpensive, but precise manner, which led to this study.

Sandy pastures under Brazilian Cerrado conditions with *Brachiaria* forage were studied due to their high SOC sequestration potential. A higher Net Primary Productivity (NPP) increases SOC due to higher carbohydrate

assimilation, which is partly stored in the soil. Hodgson (1990) considers, that LAI is one of the two variables, which represent a major consistence in relation to pasture NPP. Therefore this study explored the correlation between SOC and IAF. According to Asner (1998), LAI represents, together with the LAD (Leaf Angle Distribution), the dominant control on canopy reflectance. Furthermore it is legitimate to interpret subsoil information (e.g. SOC.) by the use of upper soil surface characteristics (e.g. LAI) with satellite images, if there is a strong correlation among them. Several studies point out a good relationship between the IAF and spectral vegetation indexes (SVIs) as the Normalized Difference Vegetation Index (NDVI) (e.g. Broge & Leblanc, 2000). As the SVIs can be expressed in satellite images, SOC estimation based on IAF determination by satellite images seems to be a promising approach, if a significant correlation between these two parameters can be found. Several studies also explored the relationship between soil organic matter and soil reflectance (e.g. Henderson et al., 1989). By so far there exists very little research about the spectral relationship between subsurface SOC combined with vegetation/soil reflectance at orbital remote sensing scale. The objective of this study is to explore this relationship, taken into account,

that SOC estimation by orbital remote sensing has mainly to deal with partly or fully plant covered areas.

## 2. MATERIAL AND METHODS

### 2.1 Characterization of the study site

The study sites were located in the Brazilian Cerrado, the second largest biome in South America. This vegetation comprises an intricate mosaic of land cover types, vertically structured as grassland, shrubland, and woodland. The studied pastures are situated in the county of Piracicaba (São Paulo State). It will be referred to them by their farm names (Barreiro Rico, Bondade, Descalvado and Monjelada). The climate is humid mesotermic with relative cold and dry winters (Cw according to Köppen), in which the monthly average temperature isn't above 18°C for all months (Cwa). Meteorological records of Piracicaba county indicate an annual middle temperature of 21,6°C with an annual middle precipitation of 1,166mm for the studied year 2001 (ESALQ/USP, 2003). The studied soil in all four pastures is Neossolo Quartzarênico (Brazilian soil classification), which refers to Psamments (U.S. soil taxonomy) and Arenosols (FAO classification).

### 2.2 Pasture selection

Four pastures with different productivity levels were visually chosen (and afterwards as representative validated). All four pastures feature a big enough extension (approximately two hectares) to cover entirely pixels of the satellite image, to ensure a spectral response that is exclusively related to pasture without interferences of other land uses. The pixel of a Landsat 7 image represents 30m of width and length, which leads to minimum extension of 3x3 pixels (90x90m) to ensure an exclusive pasture pixel in the middle of the kernel.

### 2.3 SOC of the pastures

**2.3.1 Soil sampling** The soil was sampled by cylinders (ϕ 10cm) at following soil depths:

**0 – 5 cm / 5 –10 cm / 10 – 20 cm / 20 – 30 cm / 30 –40 cm / 40-50 cm**

The soil was horizontally collected for each layer and pasture by six repetitions, except the 0-5cm-layer (8 repetitions), to account for higher spatial variety of carbon in the uppermost layer.

**2.3.2 Carbon analysis** The samples were dried three days at 60 °C. Before weighing the samples, the gross roots were removed. The samples were sub-sampled by successive diagonal halving, maintaining a representative sub-sample. Fine roots were removed from the sub-sample, considering the recent endeavors to produce more precisely SOC measures. Therefore, a plastic ruler was electro statically charged and held over the sub-sample. The electrostatics removed exclusively the fine roots without soil particles. The carbon content of the sub-samples was determined by dry combustion in a carbon analyzer (LECO CN-2000).

**2.3.3 SOC calculation** The SOC stocks were calculated as following:

$$\text{SOC (Mg ha}^{-1}\text{)} = \text{carbon (\%)} \cdot \text{bulk density (g/m}^3\text{)} \cdot \text{depth of soil layer (cm)} \div 100 \text{ (conversion factor \%)} \cdot 100 \text{ (conversion factor g/m}^3\text{ into Mg ha}^{-1}\text{)}$$

### 2.4 LAI of the pastures

The LAI-sampling was done in the transition period from wet to dry season. In this time of year, the less productive pastures start to suffer water stress, affecting the photosynthetic activity of the pasture, which leads to higher differences of LAI in between pastures. The sampling was done by a ring, covering 0,25m<sup>2</sup>. The samples were randomly taken in May 30/31 in 2001, with 8 repetitions for each pasture. The litter inside of the ring was removed, followed by an entire cut of the green biomass. The samples were immediately weighted due to minimizing humidity losses; hereupon approximately 20% of the entire sample was extracted and immediately weighted, to constitute a representative sub-sample. Subsequently, the sub-samples were separated in two fractions: green leaves and remaining parts. The green leaves were measured by a Leaf Area Meter (LI-COR: LI-3100). The LAI of the entire sample was calculated as following:

$$\text{LAI}_{\text{entire sample}} = \frac{\text{Fresh Weight}_{\text{entire sample}}}{\text{Fresh Weight}_{\text{sub-sample}}} \cdot \text{LAI}_{\text{sub-sample}}$$

### 2.5 Spectral behavior of the pastures

**2.5.1 Satellite Image** The study used a satellite image of Landsat 7 (World Reference System: 220/76), which represents one of the global standards in remote sensing of terrestrial resources (USGS, 1999). The sensor ETM+ of Landsat 7 features following spectral characteristics:

Principal Characteristics of Landsat 7				
Band 1	2	3	4	
Bandwidth (µm):	0.45 – 0.52	0.53 – 0.61	0.63 – 0.69	0.78 – 0.90
Spatial resolution:				
30m	30m	30m	30m	
Band 5	6	7	8	
Bandwidth (µm)	1.55 – 1.75	10.4 – 12.5	2.09 – 2.35	0.52 – 0.90
Spatial resolution:				
30m	30m	60m	15m	

Table 1. Characteristics of the spectral bands of Landsat 7 (USGS, 1999)

**2.5.2 Image Processing** Before processing, a sub-image (~35x12km) was extracted from the entire scene to enable more precise georeferencing and processing speed. This sub-image was then geometrically and radiometrically corrected. It was georeferenced by 12 Ground Control Points (GCP), taken by a differential GPS system (GeoExplorer II / Trimble); the precision error of the used system is under 1m (Trimble, 1999), which is considered adequate for the study task. The GCPs were taken in locations, which were easily recognizable on the satellite image, to assure precise georeferencing. The GCPs were imported into a GIS (Geographic Information System), in which the georeferencing was compiled, using an order 3 polynomial model. The sub-image was atmospherically corrected by an atmospheric correction software (ATCOR-2). The extensions of the studied pastures were marked out by DGPS. The GCPs of the pastures were imported into a GIS (TNTmips) and transformed into polygons, to extract the pastures as raster objects from the sub-image.

**2.5.3 Conversion of DNs into reflectance** The digital numbers (DN) of the grayscale raster image were converted into surface reflectance (in %). First, the DNs were converted

into apparent radiance by the following formula (Markham & Barker, 1986):

$$\text{RAD}(\lambda) = (\text{Lmax} \lambda - \text{Lmin} \lambda) 255^{-1} \cdot \text{DN} + \text{Lmin} \lambda$$

where  $\text{RAD}(\lambda)$  = spectral radiance ( $\text{W} \cdot \text{m}^{-2} \cdot \text{ster}^{-1} \cdot \mu\text{m}^{-1}$ )

$\text{Lmin} \lambda$  = spectral radiance range minimum (high gain)

$\text{Lmax} \lambda$  = spectral radiance range maximum (high gain)  $\text{DN}$  = digital number of the considered pixel

Hereupon, the apparent radiance values were converted into reflectance by the following formula (Moreira, 2001):

$$\rho = \pi \cdot \text{RAD} \lambda \cdot d^2 \cdot \text{Esol} \lambda^{-1} \cdot \cos \theta s^{-1}$$

where  $\rho$  = top of (planetary) reflectance,  $\text{RAD} \lambda$  = spectral radiance at the sensor's aperture ( $\text{W} \cdot \text{m}^{-2} \cdot \text{ster}^{-1} \cdot \mu\text{m}^{-1}$ )

$d$  = earth-sun distance, in astronomical units: 1,0109 for the 10<sup>th</sup> of may (NASA, 2003)

$\text{Esol} \lambda$  = mean solar irradiance ( $\text{W} \cdot \text{m}^{-2} \cdot \mu\text{m}^{-1}$ ) (NASA, 2003),  $\theta s$  = solar zenith angle ( $50,6^\circ$ )

**2.5.4 Comparative Statistical Analysis** A linear regression analysis was performed to determine the correlation degree between SOC/LAI and SOC/spectral reflectance of the pastures. Correlation degrees with 95% or higher were considered significant and were plotted in this article.

### 3. RESULTS AND DISCUSSION

#### 3.1 LAI of pastures

Figure 1. Leaf Area Index of the four pastures

The four pastures show differences in LAI, ranging from 0,150 to 1,103m<sup>2</sup>/m<sup>2</sup>, which refers to 635% higher LAI for the pasture with the highest LAI compared to the lowest. The overall low LAI levels of the four pastures are associated to their sandy soil texture. The LAI differences between the four pastures are mainly the result of different management practices as the bio-physical factors, which influence the LAI, are very similar among all pastures (same soil type, forage, climate, topography). The management practices differ in manuring and overgrazing. The two pastures with lower LAI have no manuring and the pasture with the lowest LAI also suffers overgrazing. The high standard deviation of pasture Bondade is related to a not entirely plant cover, showing partly bare soil spots.

#### 3.2 SOC of pastures

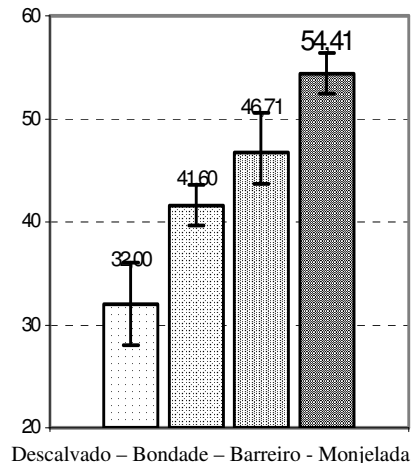


Figure 2. Soil carbon stock (SOC) of soil depth 0 -50cm

Observation: The individual soil layers (0-5, 5-10, 10-20, 20-30, 30-40 and 40-50 were treated as one soil layer 0-50cm).

The four pastures show differences in SOC, ranging from 32,0 to 54,41Mg ha<sup>-1</sup>, which refers to 70,1% more SOC in the pasture with highest SOC compared to the lowest. The overall low SOC stocks of the four pastures depend principally on their sandy soil texture. The differences in their SOC reflect different management practices, as seen for LAI differences. Both, SOC and LAI, have almost the same determining parameters (climate, soil type, native vegetation, forage specie, topography) and differ only in relation to native or former land use, which is only sensitive to SOC. The following paragraph explains this relation.

#### 3.3 Correlation between SOC and LAI

SOC and the LAI showed the expected positive correlation between each other. Both tend to have an almost linear behavior. As the IAF varies seasonally, it is of future interest to obtain the IAF from other seasons and evaluate its correlation over the year in terms of SOC (which varies seasonally very little), to define the most suited "season" for SOC/LAI correlation determination.

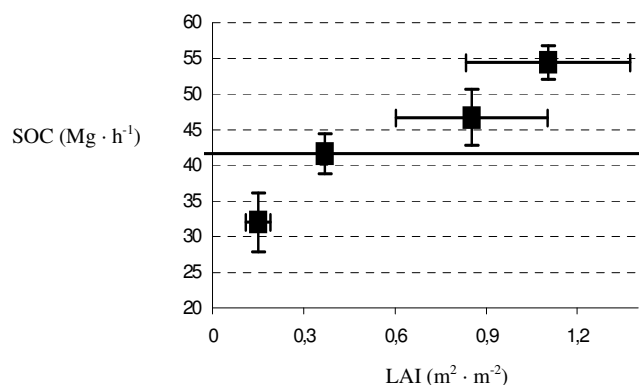


Figure 3. Correlation between SOC (Soil Organic Carbon) and LAI (Leaf Area Index)

Observation: The high standard deviation of Bondade refers to partly uncovered plant cover at this site

### 3.4 Regression Analysis between LAI and SOC

LAI = a + b SOC			
	estimate of the equation	standard error	p < 0,5
a	- 1,336	0,367	0,068
b	0,045	0,008	0,032; *
r	<b>0,97</b>		<b>0,033; *</b>

Table 2. Linear regression between SOC and LAI

where a = intersection with the y-axis  
 b = gradient  
 r = correlation coefficient  
 \* = significant correlation with p < 0,5

The correlation coefficient **r (0,97)** indicates a significant correlation between SOC and LAI, with reliability over 95%.

### 3.5 Pasture reflectance

#### 3.5.1 Conversion of DNs into reflectance

Band	Exo-atmospheric reflectance (ρ) (%)			
	Monjelada	Barreiro R.	Bondade	Descalvado
Blue	<b>9,13 ± 0,38</b>	<b>10,0 ± 0,36</b>	<b>10,46 ± 0,37</b>	<b>10,55 ± 0,31</b>
Green	<b>8,31 ± 0,61</b>	<b>9,48 ± 0,48</b>	<b>9,55 ± 0,50</b>	<b>9,30 ± 0,34</b>
Red	<b>6,11 ± 0,87</b>	<b>8,19 ± 1,08</b>	<b>9,61 ± 0,80</b>	<b>10,33 ± 0,75</b>
NIR	<b>25,51 ± 2,10</b>	<b>30,13 ± 1,87</b>	<b>22,66 ± 1,60</b>	<b>20,17 ± 1,02</b>
SWIR I	<b>17,92 ± 2,39</b>	<b>23,18 ± 2,33</b>	<b>27,16 ± 2,01</b>	<b>28,38 ± 2,44</b>
SWIR II	<b>6,17 ± 1,46</b>	<b>8,81 ± 1,92</b>	<b>14,42 ± 2,06</b>	<b>14,58 ± 1,90</b>

Table 3. Conversion of DNs into planetary reflectance  
 Observation: the value ± refers to the standard deviation

**3.5.2 Regression analysis between SOC and pasture reflectance** The following table shows the results of the linear regression analysis between SOC and six spectral bands.

Reflectance =	a	+	b	· SOC	r
Blue	(12.8 ± 0.9)	+	(- 0.06 ± 0.02)	· SOC	0.91
Green	(4.4 ± 0.6)	+	(- 0.02 ± 0.01)	· SOC	0.64
Red	(16.8 ± 1.8)	+	(- 0.19 ± 0.04)	· SOC	<b>0.96</b>
NIR	(11.1 ± 10.4)	+	(0.31 ± 0.25)	· SOC	0.68
SWIR I	(44.9 ± 5.2)	+	(-0.47 ± 0.12)	· SOC	<b>0.95</b>
SWIR II	(28.7 ± 5.8)	+	(-0.41 ± 0.13)	· SOC	0.91

Table 4. Linear regression between SOC and pasture reflectance

where a = intersection with the y-axis  
 b = gradient, r = correlation coefficient

Two correlation coefficients (r) were equal or higher than 0.95, indicating a significant correlation with a probability of at least 95%; therefore these two correlations (red band/SOC and SWIR I/SOC) were plotted and discussed in detail.

### 3.5.3 Correlation between SOC and pasture reflectance in the red spectrum

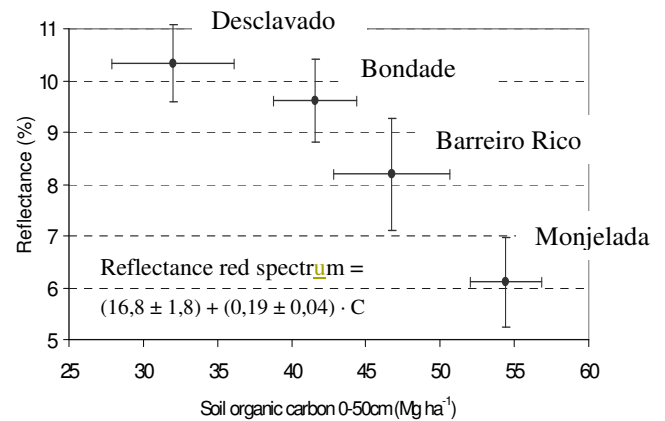


Figure 4. Correlation between SOC and reflectance in the red spectrum of the studied pastures

Observations: The average reflectance of each pasture is acquired by following pixel number: (217 Monjelada, 495 Barreiro Rico, 89 Bondade e 89 Descalvado).

The SOC is considered a strong factor of influence in terms of soil reflection. The higher the SOC, the fewer the reflectance in the wavelength spectra visible to short wave (Major et al., 1992), as can be seen in figure x. The soil reflectance of the studied pastures is likely to be the same, as the studied pastures feature the same soil type, climate, topography and a closed vegetation cover (except Bondade). This leads to the assumption, that the in figure x plotted differences in pasture reflectance are mainly linked to differences in plant reflectance. The red spectra suffer radiative absorption by the photosynthetically active pigments chlorophyll a (absorption max. 675nm) and b (absorption max. 480nm) in the green leaves. Therefore, the photosynthetically absorption pattern are responsible for the different reflectance of the studied pastures in the red spectrum.

### 3.5.4 Correlation between SOC and pasture reflectance in the shortwave infrared I spectrum

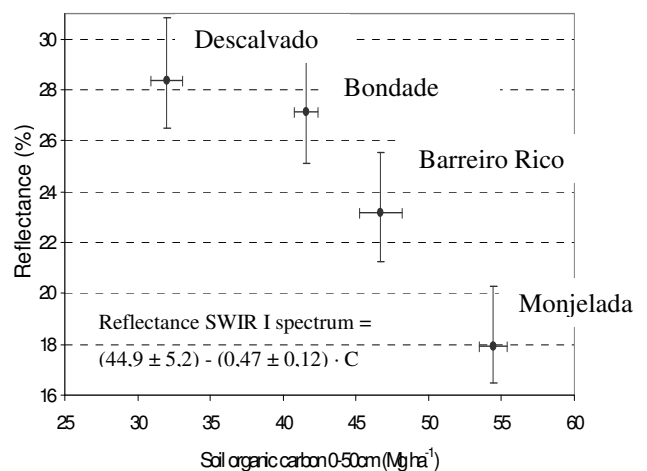


Figure 5. Correlation between SOC and reflectance in the shortwave I infrared spectrum (1550 - 1750nm) of the studied pastures

Physical-based studies have shown that shortwave infrared (SWIR) (1400–2500 nm) is strongly influenced by the water in plant tissue (Gausman, 1984). In particular, the wavelengths at 1530 and 1720 nm seem to be most appropriate for assessing vegetation water (Fourty & Baret, 1998). The water fills out the cavities, forming a more liquid environment inside the leaf. With this, occurs a decreasing of the differences of the refraction index between the air and the hydrated cell wall, which increases its transmittance and decreases the reflectance (Moreira, 2001). Therefore the here shown results express, inter alia, mainly the differences in plant water content for the four pastures. This leads to the assumption that vegetal water content, which is linked to productivity, is responsible for the second highest correlation coefficient between reflectance spectra and SOC.

#### 4. CONCLUSIONS

Due to the urge of reliable, fast and inexpensive SOC estimation in accordance with environmental politics as the Kyoto Protocol, the study evaluated the potential of orbital remote sensing for this purpose.

It was observed a good correlation ( $r = 0,97$ ) between SOC and LAI. Several studies point out, that the LAI can be calculated in satellite images by the NDVI (e.g. Friedl, 1997). Under this assumption, the good correlation between SOC and LAI leads to the promising approach to estimate current and potential SOC by remotely sensed LAI determination.

Furthermore was identified an also good correlation between SOC and some spectra of pasture reflectance. A regression analysis showed particularly good correlations in the red ( $r = 0,96$ ) and shortwave infrared I ( $r = 0,95$ ) spectra. The red spectrum refers mainly to photosynthesis activity and the SWIR I spectrum to waterleaf content of the pastures. The good correlations in these two spectra with SOC lead to the conclusion, that photosynthesis activity and waterleaf content, that are detectable by orbital remote sensing, can be linked to SOC. It is of interest to investigate these three shown correlations of LAI, red and SWIR I spectrum in relation to SOC in time and space under similar and different circumstances to verify its validation and study the possibilities of its applicability for different pasture or other land use settings.

#### REFERENCES

- Asner, G.P., 1998. Biophysical and biochemical sources of variability in canopy reflectance. *Remote Sensing of Environment*, (64)3, pp. 234-253.
- Broge, N.H.; Leblanc, E., 2001. Comparing prediction power and stability of broadband and hyperspectral vegetation indices for estimation of green leaf area index and canopy chlorophyll density. *Remote Sensing of Environment*, (76,)2, pp. 156-172.
- Escola Superior de Agricultura “Luiz de Queiroz” (ESALQ/USP) Base de dados da estação meteorológica automatizada. <http://ce.esalq.usp.br/dce/postoaut.htm> (28 Aug. 2003).
- Fourty, T.; Baret, F, 1998. On spectral estimates of fresh leaf biochemistry. *International Journal of Remote Sensing*, (19)7, pp. 1283-1297.

- Friedl, M.A., 1997. Examining the effects of sensor resolution and sub-pixel heterogeneity on spectral vegetation indices: Implications for biophysical modeling. In: *Scale in remote sensing and GIS*. Boca Raton: Lewis Publications, pp.125-139.
- Gausman, H.W.; Burke, J.J.; Quisenberry, J.E., 1984. Use of leaf optical-properties in plant stress research. *ACS Symposium Series*, (257), pp. 215-233.
- Henderson, T.L.; Szilagyi, A.; Baumgardner, M.F.; Chen, C.C.T. & Landgrebe, D.A., 1989. Spectral band selection for classification of soil organic-matter content. *Soil Science Society of America Journal*, (53)6, pp. 1778-1784.
- Hodgson, J.G., 1990. *Grazing management – science into practice*. Longman Scientific and Technical, Essex, 203p.
- Intergovernmental Panel On Climate Change (IPCC), 2000. *Land use, land-use change, and forestry special report*. Cambridge: IPCC.
- Markham, B.L.; Barker, J.L., 1986. Landsat MSS and TM postcalibration on dynamic ranges of exoatmospheric reflectances and at satellite temperatures. EOSAT (Landsat Technical Notes, 1), Lanham.
- Major, D.J.; Janzen, H.H.; Olson, B.M.; Mc Ginn, S.M., 1992. Reflectance characteristics of Southern Alberta soils. *Canadian Journal Of Soil Science*, (72)4, pp. 611-615.
- Moreira, M.A., 2001. Fundamentos do sensoriamento remoto e metodologias de aplicação. Com Deus, São José dos Campos.
- NASA. *Landsat 7 science data users handbook*. chapter11. [http://ltpwww.gsfc.nasa.gov/IAS/handbook/handbook\\_htmls/chapter11/chapter11.html](http://ltpwww.gsfc.nasa.gov/IAS/handbook/handbook_htmls/chapter11/chapter11.html) (03.02.2003).
- Trimble Navigation Limited., 1999. Characterizing accuracy of Trimble Pathfinder mapping receivers.
- US Geological Survey (USGS) 1999. Landsat 7 Datasets Document. [http://eosims.cr.usgs.gov:5725/DATASET/landsat7\\_dataset.html](http://eosims.cr.usgs.gov:5725/DATASET/landsat7_dataset.html) (accessed 03 Feb. 2003).
- Walsh, M.J., 1999. Maximizing financial support for biodiversity in the emerging Kyoto protocol markets. *The Science of the Environment*, (240), pp. 145-156.

#### ACKNOWLEDGEMENTS

The authors thank for the research support, provided by Conselho Nacional de Desenvolvimento Científico, Brazil (CNPq) with Grant No. 133344-2000-2 and financial support by the Institut de Recherche pour le Développement (IRD), France